Introduction to Small-Angle Neutron Scattering and Neutron Reflectometry

Andrew J Jackson
NIST Center for Neutron Research

May 2008

Contents

1 Introduction

The neutron is a spin 1/2 sub-atomic particle with mass equivalent to 1839 electrons (1.674928×10^{-27} kg), a magnetic moment of -1.9130427 μ_n ($-9.6491783\times10^{-27}\mathrm{JT}^{-1}$) and a lifetime of 15 minutes (885.9 s).

Quantum mechanics tells us that, whilst it is certainly particulate, the neutron also has a wave nature and as such can display the gamut of wave behaviors including reflection, refraction and diffraction.

This introduction covers briefly the theory of neutron scattering and that of two techniques that make use of the wave properties of neutrons to probe the structure of materials, namely *small angle neutron scattering* (diffraction) and *neutron reflectometry* (reflection and refraction).

Since this introduction is exactly that, the reader is encouraged to look to the extensive literature on the subject and a recommended reading list is provided at the end. Much of the material presented here has been taken from those references.

2 Neutron Scattering

2.1 Neutron-nucleus interaction

The scattering of neutrons occurs in two ways, either through interaction with the nucleus (*nuclear scattering*) or through interaction of unpaired electrons (and hence the resultant magnetic moment) with the magnetic moment of the neutron (*magnetic scattering*). It is the former of these that this introduction will address.

Let us consider the *elastic* scattering of a beam of neutrons from a single nucleus. In this case we treat the nucleus as being rigidly fixed at the origin of coordinates and there is no exchange of energy (Figure (1)). The scattering will depend upon the interaction potential $V(\mathbf{r})$ between the neutron and the nucleus, separated by $\mathbf{r}$. This potential is very short range and falls rapidly to zero at a distance of the order of 10^{-15} m. This is a much shorter distance than the wavelength

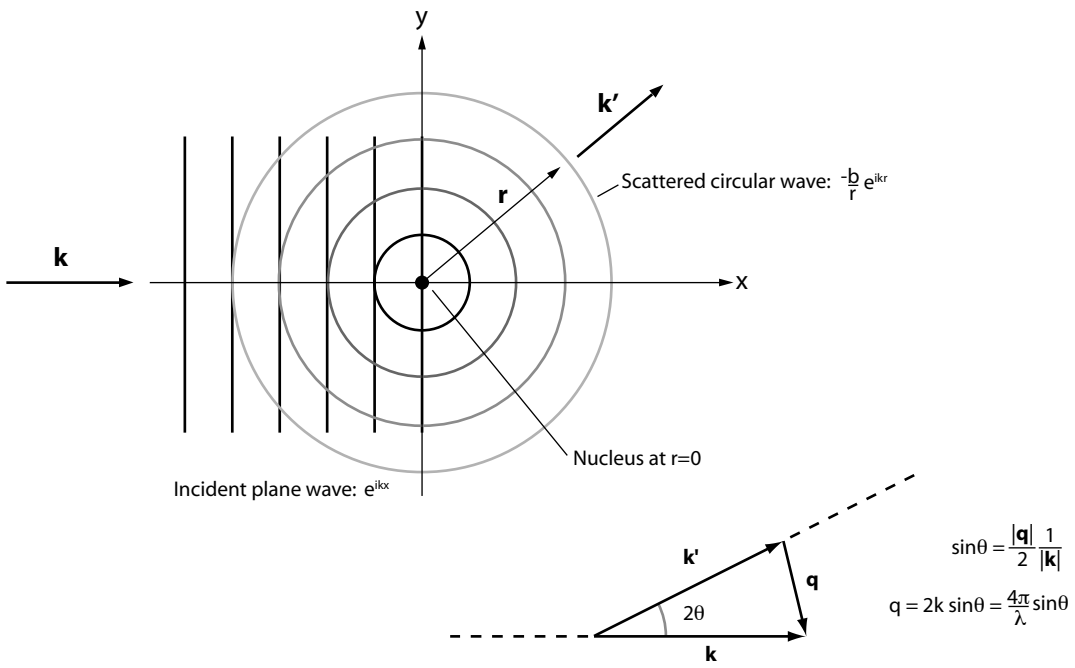

Figure 1: Elastic neutron scattering from a fixed nucleus (after Pynn, 1990)

of the neutrons which is of the order of 1Å (10^{-10} m) and as a result the nucleus acts as a point scatterer.

We can represent the beam of neutrons by a plane wave with wavefunction

$$\Psi_i = e^{ikz} \tag{1}$$

where z is the distance from the nucleus in the propagation direction and $k = 2\pi/\lambda$ is the wavenumber. The scattered wave will then be spherically symmetrical (as a result of the nucleus being a point scatterer) with wavefunction

$$\Psi_s = -\frac{b}{r}e^{ikr} \tag{2}$$

where b is the *nuclear scattering length* of the nucleus and represents the interaction of the neutron with the nucleus. The minus sign is arbitrary and is used so that a positive value for b indicates a repulsive interaction potential. The scattering length is a complex number, but the imaginary component only becomes important for nuclei that have a high absorption coefficient (such as boron and cadmium) and it can otherwise be treated as a real quantity.

The scattering length of nuclei varies randomly across the periodic table. It also varies between isotopes of the same element. A useful example of this is ^{1}H and ^{2}H (hydrogen and deuterium respectively with the latter often labeled D). Hydrogen has a coherent (see later section) scattering length of -3.74×10^{-5}Å and deuterium 6.67×10^{-5}Å. Thus the scattering length of a molecule can

be varied by replacing hydrogen with deuterium and potentially be made to match that of some other component in the system. This technique of *contrast variation* is one of the key advantages of neutron scattering over x-rays and light.

As mentioned above, the neutron can also interact with the magnetic moment of an atom. This magnetic interaction has a separate *magnetic scattering length* that is of the same order of magnitude, but independent from, the nuclear scattering length. Thus, for example, one can use contrast variation to remove the nuclear component of the scattering and leave only the magnetic. The magnetic interaction is spin-dependent, so it is also possible to extract information about the magnetization through the use of polarized neutrons. These advanced uses are beyond the scope of this introduction, but more information can be found in the reference material listed at the end.

Having treated the case of a single nucleus, if we now consider a three-dimensional assembly of nuclei whilst maintaining the assumption of elastic scattering the resultant scattered wave will then be

$$\Psi_s = -\sum_i \left(\frac{b_i}{r}\right) e^{ikr} e^{i\mathbf{q}\cdot\mathbf{r}} \tag{3}$$

where $\mathbf{q} = \mathbf{k_i} - \mathbf{k_s}$ and is known as the *scattering vector* with $\mathbf{k_i}$ and $\mathbf{k_s}$ being the wavevectors of the incoming and scattered neutrons respectively.

2.2 Scattering Cross Section

The scattering cross section is a measure of how "big" the nucleus appears to the neutron and thus how strongly neutrons will be scattered from it.

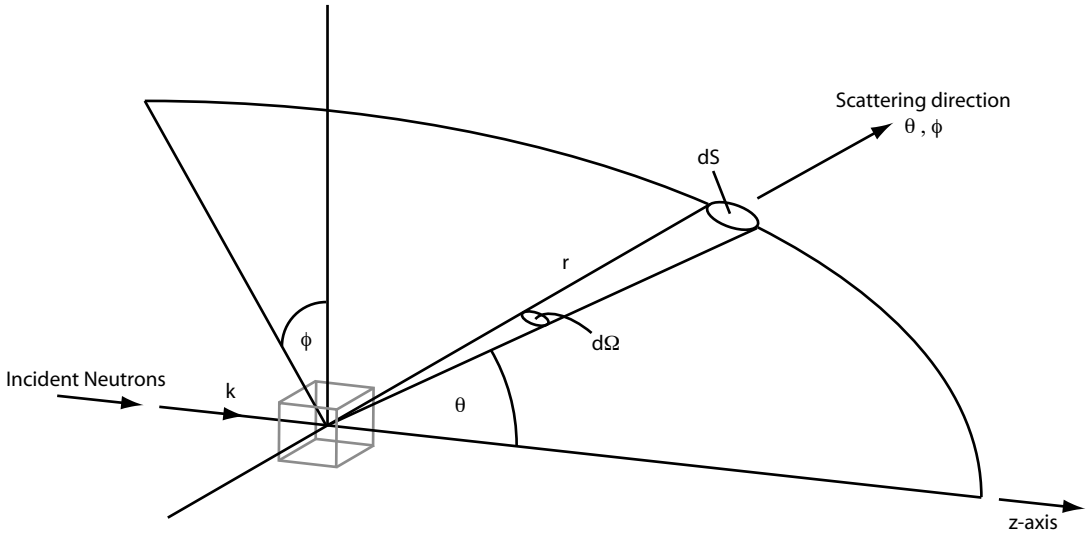

Figure 2: The geometry of a scattering experiment (after Squires)

Imagine a neutron scattering experiment where a beam of neutrons of a given energy E is incident

on a general collection of atoms (your sample - it could be a crystal, a solution of polymers, a piece of rock, etc) (Figure 2). If we again assume elastic scattering (such that the energy of the neutrons does not change) we can set up a neutron detector to simply count all the neutrons scattered into the solid angle $d\Omega$ in the direction θ, ϕ. The *differential cross section* is defined by

$$\frac{d\sigma}{d\Omega} = \frac{\text{number of neutrons scattered per second into } d\Omega \text{ in direction } \theta, \phi}{\Phi d\Omega} \tag{4}$$

where Φ is the number of incident neutrons per unit area per second, referred to as the incident flux. The name "cross section" suggests that this represents an area and indeed, we can see that the dimensions of flux are [area^{-1} time^{-1}] and those of the numerator in equation (4) are [time^{-1}] resulting in dimensions of [area] for the cross section.

The *total scattering cross section* is defined by the equation

$$\sigma_s = \frac{\text{total number of neutrons scattered by second}}{\Phi} \tag{5}$$

and is related to the differential scattering cross section by

$$\sigma_s = \int \frac{d\sigma}{d\Omega} d\Omega \tag{6}$$

The cross section is the quantity that is actually measured in a scattering experiment and the basic problem is to derive theoretical expressions that describe it for given systems of scatterers. Experimentally the cross sections are usually quoted per atom or per molecule and thus the definitions above are then divided by the number of atoms or molecules in the scattering system.

We can calculate the cross section $d\sigma/d\Omega$ for scattering from a single fixed nucleus using the expressions given above. Denoting the velocity of the neutrons as v and again treating elastic scattering, the number of scattered neutrons passing through an area dS per second is

$$v dS |\psi_s|^2 = v dS \frac{b^2}{r^2} = v b^2 d\Omega \tag{7}$$

The incident neutron flux is

$$\Phi = v|\psi_i|^2 = v \tag{8}$$

From equation (4)

$$\frac{d\sigma}{d\Omega} = \frac{v b^2 d\Omega}{\Phi d\Omega} = b^2 \tag{9}$$

and then integrating over all space (4π steradians) we obtain

$$\sigma_{tot} = 4\pi b^2 \tag{10}$$

We can perform a similar calculation for the assembly of nuclei whose wavefunction was given in equation (3) above and obtain the differential cross section

$$\frac{d\sigma}{d\Omega}(\mathbf{q}) = \frac{1}{N} \left| \sum_i^N b_i e^{i\mathbf{q}\cdot\mathbf{r}} \right|^2 \tag{11}$$

which we can now see is a function of the scattering vector, $\mathbf{q}$.

2.3 Coherent and Incoherent Cross Sections

The above discussion applies to the case where there is only one isotope of one element present (specifically an element with zero nuclear spin), however practically all real systems will have a distribution of both elements and isotopes of those elements. The result of this distribution is that the total cross section is, in fact, a sum of two components a *coherent* part and an *incoherent* part

$$\sigma_{tot} = \sigma_{coh} + \sigma_{incoh} \tag{12}$$

The coherent scattering cross section, σ_{coh}, represents scattering that can produce interference and thus provides structural information. Conversely, the incoherent cross section does not contain structural information. The two are related to the mean and variance of the scattering length such that

$$\sigma_{coh} = 4\pi < b >^2 \text{ and } \sigma_{incoh} = 4\pi(< b^2 > - < b >^2) \tag{13}$$

The total scattering cross section is then

$$\sigma_s = 4\pi < b^2 > \tag{14}$$

We previously learned that the scattering length b is, in fact, a complex number. If we take account of the imaginary part, which represents the absorption, then the *total scattering cross section* becomes

$$\sigma_{tot} = \sigma_s + \sigma a \sigma_{tot} = \sigma_{coh} + \sigma_{incoh} + \sigma_a \tag{15}$$

where σ_a is the *absorption cross section.*

3 Small Angle Neutron Scattering

The discussion above focussed on atomic properties, but there are many problems where the length scales in question are much larger than atomic dimensions and it is easier to think in terms of material properties. In order to do this we define a quantity called the *scattering length density*

$$\rho(\mathbf{r}) = b_i \delta(\mathbf{r} - \mathbf{r_i}) \tag{16}$$

or

$$\rho = \frac{\sum_i^n b_i}{\overline{V}} \tag{17}$$

where ρ is the scattering length density, b_i is the scattering length of the relevant atom and $\overline{V}$ is the volume containing the n atoms.

This is a much more useful way to think about materials science problems, but can we really replace the atomic properties in this way? Consider the case of water. If we calculate the scattering length density as a function of radius from a given oxygen atom (Figure (3)) we can see that beyond a certain radius r^* the scattering length density becomes constant and so above $q = 1/r^*$ the details of the atomic structure are lost and the scattering length density is a valid description.

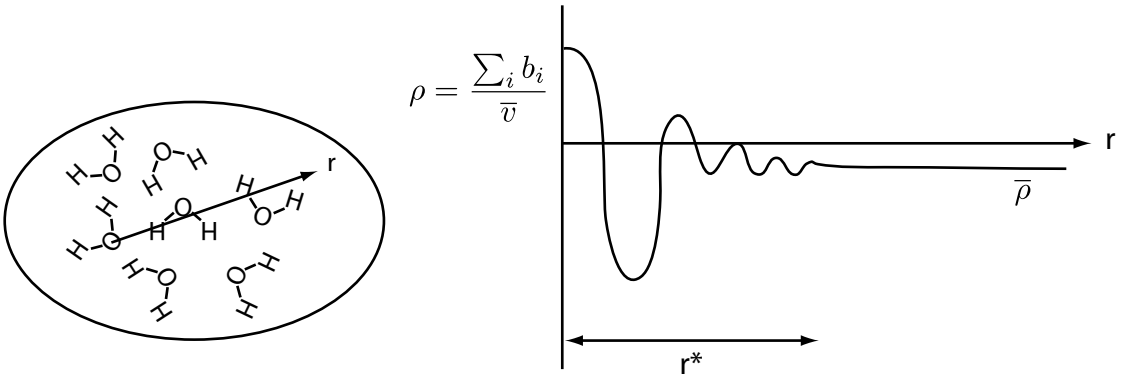

Figure 3: Scattering length density of water as a function of distance from a given oxygen atom (after Kline)

So, we can now make the replacement of the sum in

$$\frac{d\sigma}{d\Omega}(\mathbf{q}) = \frac{1}{N}\left|\sum_i^N b_i e^{i\mathbf{q}\cdot\mathbf{r}}\right|^2 \tag{18}$$

by the integral of the scattering length density distribution across the whole sample and normalize by the sample volume

$$\frac{d\Sigma}{d\Omega}(\mathbf{q}) = \frac{N}{V}\frac{d\sigma}{d\Omega}(\mathbf{q}) = \frac{1}{V}\left|\int_V \rho(\mathbf{r})e^{i\mathbf{q}\cdot\mathbf{r}}d\mathbf{r}\right|^2 \tag{19}$$

This result is known as the "Rayleigh-Gans Equation" and shows us that small angle scattering arises as a result of *inhomogeneities in scattering length density* ($\rho(\mathbf{r})$). $\Sigma = \sigma/V$ is known as the *macroscopic cross section*. The integral term is the Fourier transform of the scattering length density distribution and the differential cross section is proportional to the square of its amplitude. This latter fact means that all phase information is lost and we cannot simply perform the inverse Fourier transform to get from the macroscopic cross section back to the scattering length density distribution.

As discussed previously, the differential cross section $d\sigma/d\Omega$ is the directly measured quantity in a scattering experiment. In the case of small angle scattering the results are usually normalized by the sample volume to obtain the result on an "absolute" scale as this permits straightforward comparison of scattering from different samples. Thus the differential macroscopic cross section is used as defined by the Rayleigh-Gans equation above.

As with the atomic cross section, the macroscopic cross section has three components

$$\frac{d\Sigma}{d\Omega}(\mathbf{q}) = \frac{d\Sigma_{coh}}{d\Omega}(\mathbf{q}) + \frac{d\Sigma_{inc}}{d\Omega} + \frac{d\Sigma_{abs}}{d\Omega} \tag{20}$$

Information about the distribution of matter in the sample is contained in the coherent component, whilst the incoherent component is not q-dependent and contributes only to the noise level. The absorption component is usually small and simply reduces the overall signal.

Whilst different types of system have different natural bases for the distribution of scattering length density, all are fundamentally equivalent - we just use different ways to describe them. In the case of particulate systems where we have "countable" units that make up the scattering, we can think about the spatial distribution of those units such that

$$\left| \int_V f(\mathbf{r}) d\mathbf{r} \right|^2 \longrightarrow \sum_i^N \sum_j^N f(\mathbf{r_i} - \mathbf{r_j}) \tag{21}$$

In polymers the units might be the monomers in the chain, in proteins we might consider polypeptide subunits and in a general particulate system the individual particles (be they molecules or oil droplets) might be used.

In non-particulate systems (for example metal alloys or bicontinuous microemulsions) a statistical description may be appropriate whereby $\rho(r)$ is described by a correlation function $\gamma(r)$.

3.1 General Two Phase System

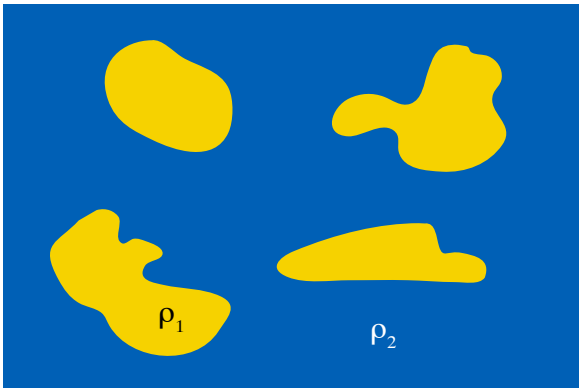

Figure 4: A system containing two phases with scattering length densities ρ_1 and ρ_2

So what is the practical result of the above discussion? Let us imagine a general two phase system such as that presented in figure 4. It consists of two incompressible phases of different scattering length densities ρ_1 and ρ_2. Thus

$$V = V_1 + V_2 \tag{22}$$

$$\rho(r) = \begin{cases} \rho_1 & \text{in } V_1 \\ \rho_2 & \text{in } V_2 \end{cases} \tag{23}$$

Taking the Rayleigh-Gans equation (equation (19)) and breaking the total volume into two sub

volumes

$$\frac{d\Sigma}{d\Omega}(\mathbf{q}) = \frac{1}{V}\left|\int_{V_1} \rho_1 e^{i\mathbf{q}\cdot\mathbf{r}} d\mathbf{r_1} + \int_{V_2} \rho_2 e^{i\mathbf{q}\cdot\mathbf{r}} d\mathbf{r_2}\right|^2 \tag{24}$$

$$\frac{d\Sigma}{d\Omega}(\mathbf{q}) = \frac{1}{V}\left|\int_{V_1} \rho_1 e^{i\mathbf{q}\cdot\mathbf{r}} d\mathbf{r_1} + \rho_2\left\{\int_{V} e^{i\mathbf{q}\cdot\mathbf{r}} d\mathbf{r} - \int_{V_1} e^{i\mathbf{q}\cdot\mathbf{r}} d\mathbf{r_1}\right\}\right|^2 \tag{25}$$

$$\tag{26}$$

So at non-zero q values

$$\frac{d\Sigma}{d\Omega}(\mathbf{q}) = \frac{1}{V}(\rho_1 - \rho_2)^2\left|\int_{V_1} e^{i\mathbf{q}\cdot\mathbf{r}} d\mathbf{r_1}\right|^2 \tag{27}$$

where the difference in scattering length densities encapsulates both material properties (density, composition) and radiation properties (scattering lengths), whilst the integral term describes the spatial arrangement of the material.

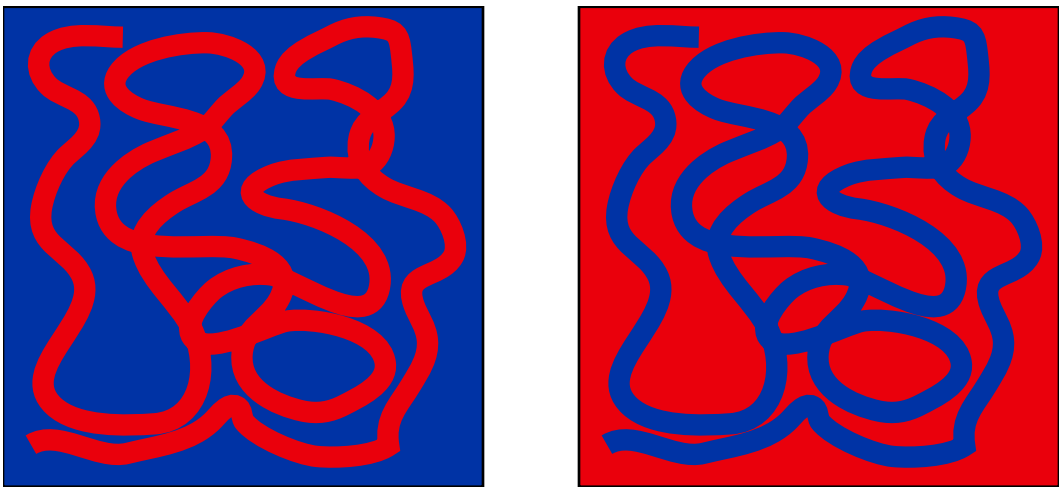

Figure 5: Two systems where the structure is the same but the scattering length densities are reversed

The above equation leads to "Babinet's Principle" that two structures, such as those shown in figure 5, which are identical other than for the interchange of their scattering length densities give the same coherent scattering (the incoherent term may be different). This is a result of the loss of phase information mentioned previously - there is no way (from a single measurement) to determine if ρ_1 is greater than ρ_2 or vice versa. Thus it is important when designing small angle scattering experiments to consider the appropriate use of *contrast variation* - usually by substitution of hydrogen for deuterium - in order to be able to solve the structure.

4 Analysis of Small Angle Scattering Data

Once the various instrumental effects have been removed and the scattering is presented as $d\Sigma/d\Omega(\mathbf{q})$ it is then necessary to perform some sort of analysis to extract useful information. Unless there is some specific orientation of scattering objects within the sample, the scattering can be averaged to give the macroscopic cross section as a function of the magnitude of $\mathbf{q}$. It is this that is most commonly presented and is known as the *1-D* small angle scattering pattern.

There are essentially two classes of analysis: model-dependent and model-independent. The former consists of building a mathematical model of the scattering length density distribution, whilst the latter consist of direct manipulations of the scattering data to yield useful information.

4.1 Model Independent Analysis

4.1.1 The Scattering Invariant

Porod showed that the total small angle scattering from a sample is a constant (i.e. invariant) irrespective of the way the sample density is distributed (figure 6).

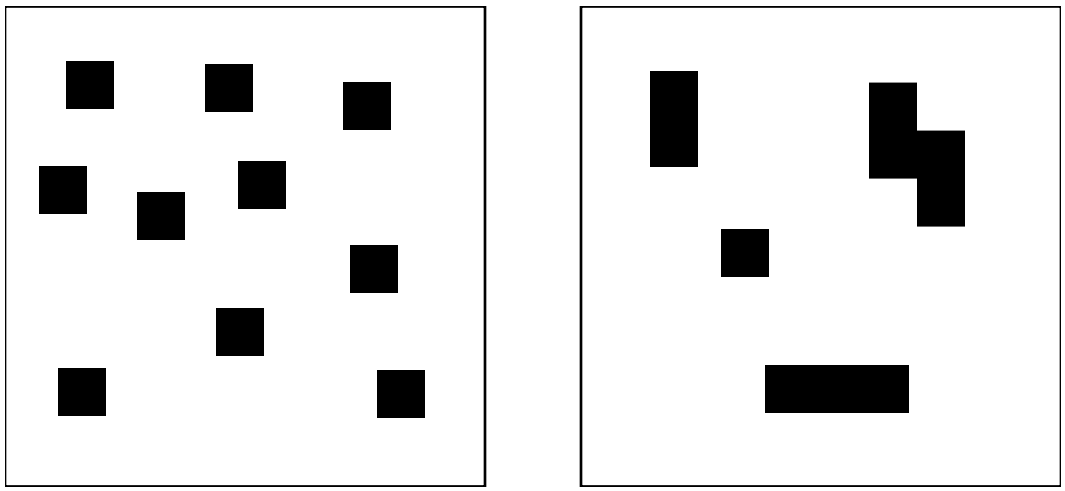

Figure 6: Two systems where the contrast and volume fraction are the same, but the distribution of matter is different. Both are 10% black and 90% white.

Integrate the differential cross section with respect to Q

$$Q = \int \frac{d\Sigma}{d\Omega}(\mathbf{q}) d\mathbf{q} \tag{28}$$

$$= (2\pi)^3 (\rho(\mathbf{r}) - \overline{\rho})^2 \tag{29}$$

and for an incompressible two-phase system

$$\frac{Q}{4\pi} = Q^* = 2\pi^2 \phi_1 (1 - \phi_1)(\rho_2 - \rho_1)^2 \tag{30}$$

Thus, in theory, this analysis allows for the calculation of the volume fraction of each component in a two-phase system given the contrast, or the contrast given the volume fractions. However in practice it is difficult to measure the scattering in a wide enough Q range to be able to calculate $Q*$.

4.1.2 Porod Scattering

Also due to Porod is a law for scattering at high values of Q (Q $\gg$ 1/D, where D is the size of the scattering object), if there are sharp boundaries between the phases of the system. The law states that at large Q

$$I(q) \propto q^{-4} \tag{31}$$

and thus

$$\frac{\pi}{Q^*} \cdot \lim_{q->\infty} (I(q) \cdot q^4) = \frac{S}{V} \tag{32}$$

where Q^* is the scattering invariant mentioned previously and S/V is the *specific surface* of the sample. If we consider the systems shown in figure 6 we can see that the specific surface of the left hand sample will be larger than that of the right hand one, but they have the same scattering invariant.

4.1.3 Guinier Analysis

Where the Porod approximation considers the high-Q limit of scattering, the low Q limit can be described using an approximation due to Guinier. The *Guinier approximation* is formulated as

$$I(Q) = I(0)e^{-\frac{(QR_g)^2}{3}} \tag{33}$$

$$ln(I(Q)) = ln(I(0)) - \frac{R_g^2}{3}Q^2 \tag{34}$$

and thus the *radius of gyration* of the scattering object, R_g, can be extracted from the slope of a plot of $ln(I(Q))$ vs Q^2, bearing in mind that the validity of the approximation is limited to values of $QR_g \ll 1$. The radius of gyration of a sphere is given by

$$R_g^2 = \frac{3}{5}R^2 \tag{35}$$

and the equations for other bodies are given in Appendix A.

4.2 Model Dependent Analysis

As we saw in the discussion of Babinet's principle, the macroscopic scattering cross section for a two phase system can be divided into a *contrast factor*, which describes the difference in scattering length density between the phases, and an integral term, which describes the spatial arrangement of the material in the phases. This latter term is the function that must be modeled.

In many cases it is possible to describe the distribution of material in terms of a *form factor*, P(q), that represents the interference of neutron scattered from different parts of the same object, and a *structure factor*, S(q), that represents the interference of neutrons scattered from different objects.

$$\frac{d\Sigma}{d\Omega}(q) = \frac{N}{V}(\rho_1 - \rho_2)^2 V_p^2 P(q) S(q) \tag{36}$$

If the system of scatterers has no interparticle correlation (e.g. it is a dilute solution) then $S(q) = 1$.

The form factor describes the size and shape of the scattering objects and analytical expressions have been derived for many common shapes such as spheres and cylinders (see below). More complex objects can usually be deduced or constructed from these.

In the case of an isotropic solution the structure factor is given by

$$S(q) = 1 + 4\pi N_p \int_0^\infty [g(r) - 1] \frac{\sin(qr)}{qr} r^2 dr \tag{37}$$

where $g(r)$ is the pair correlation function for the scattering objects and $\ln g(r)$ is directly related to the potential energy function that describes the interparticle interaction. In theory $g(r)$ can be obtained from Fourier inversion of S(q), however in practice one of the approximate forms of S(q) that have been developed for specific systems is used in model fitting.

4.2.1 The Form Factor for Spheres

For a sphere of radius r

$$P(q) = \left[\frac{3(\sin(qr) - qr\cos(qr))}{(qr)^3}\right]^2 \tag{38}$$

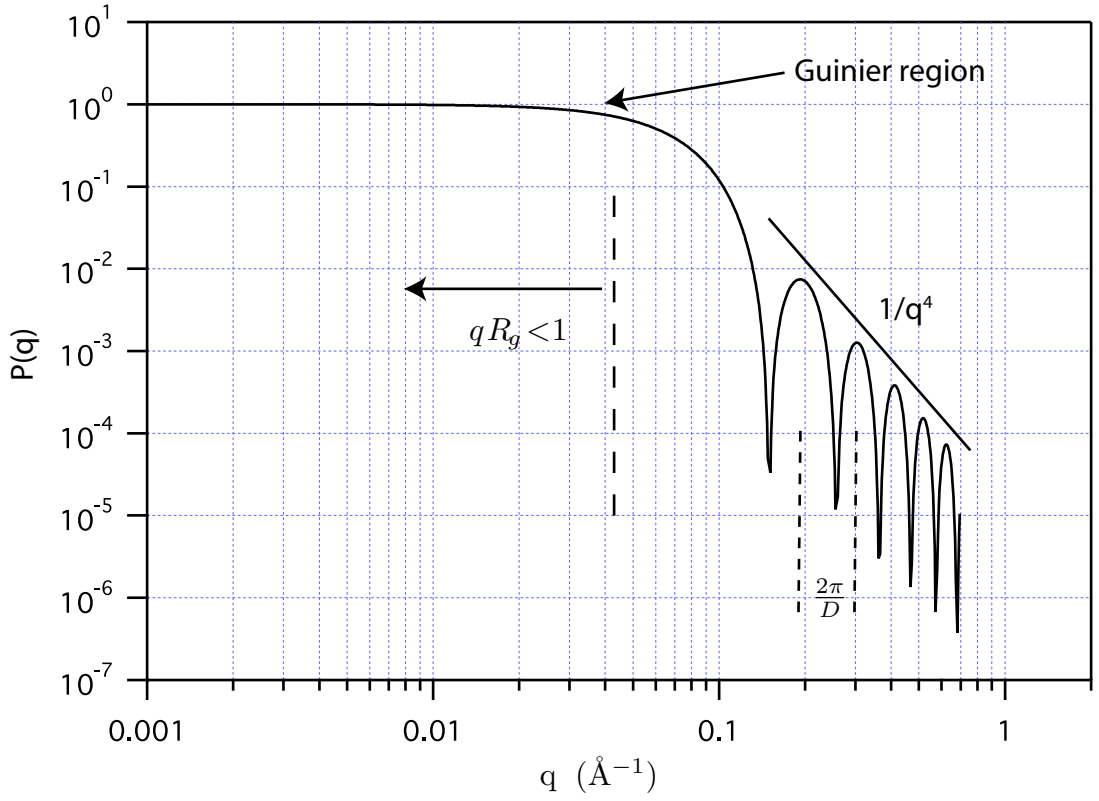

Figure 7: Form Factor spheres of radius 3Å. $R_g = 23$Å

4.2.2 The Form Factor for Cylinders

For a cylinder of radius r and length $L = 2H$

$$P(q) = \int_0^{\pi/2} f^2(q,\alpha) \sin\alpha d\alpha \tag{39}$$

$$f(q,\alpha) = j_0(qHcos\alpha)\frac{J_1(qr\sin\alpha)}{(qrsin\alpha)} \tag{40}$$

$$j_0(x) = sin(x)/x \tag{41}$$

$$V_{cyl} = \pi r^2 L \tag{42}$$

where $J_1(x)$ is the first order Bessel function. Here α is defined as the angle between the cylinder axis and the scattering vector, q. The integral over α averages the form factor over all possible orientations of the cylinder with respect to q.

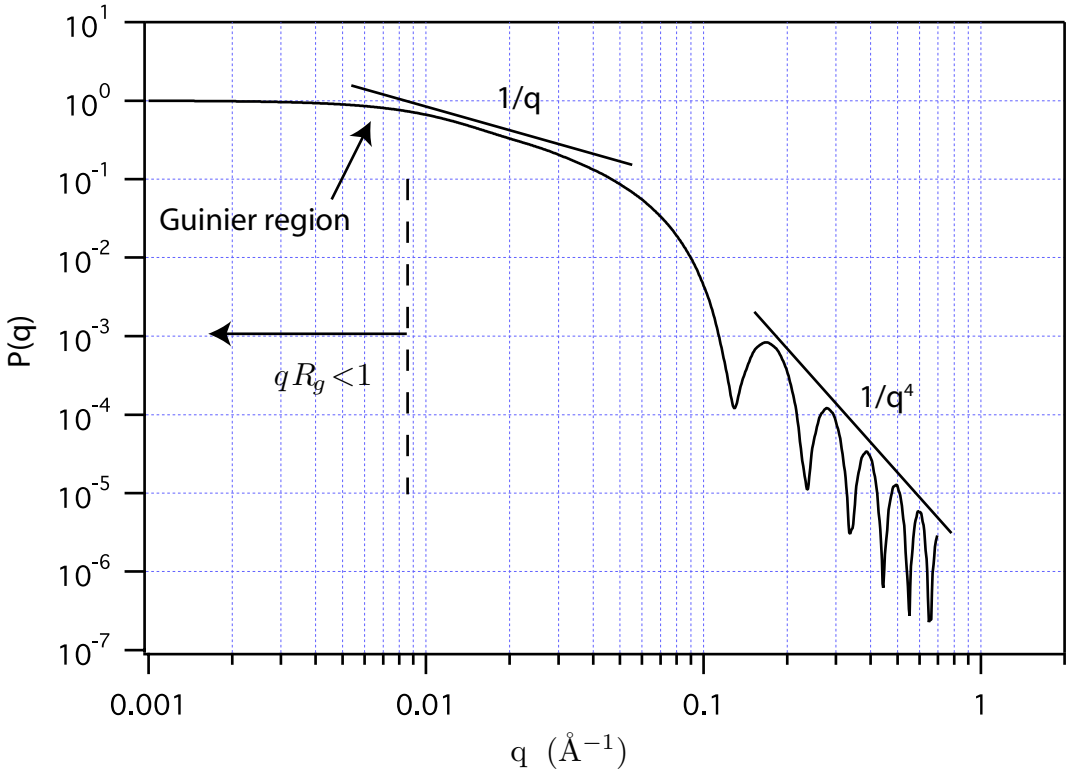

Figure 8: Form Factor for cylinders of radius 30Å and length 400Å. $R_g = 117$Å

4.3 Contrast Variation

In order to make the analysis of complex structures more tractable, the ability to vary the scattering length density through hydrogen-deuterium exchange is a key advantage of neutron scattering over other scattering techniques (x-rays, light).

Figure 9 shows an example of a core-shell type particle where contrast variation can be used to highlight various parts of the structure. The resulting scattering curves can be fitted simultaneously to the same model varying only the scattering length densities between data sets.

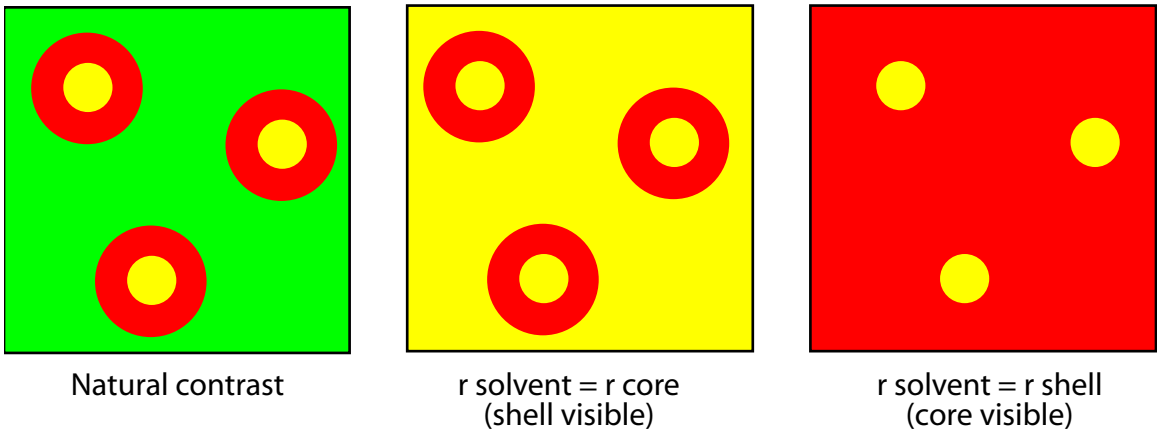

Figure 9: The effect of contrast variation on the measurable structure of a core-shell particle

4.4 Polydispersity

In real systems there is often a distribution of sizes of scattering object which has the effect of damping the high q oscillations or "smearing" the scattering curve (Figure 10). This effect can be calculated by performing an integral over the appropriate size distribution. Models that already have multiple integrals (e.g. a cylinder form factor) can become computationally intense when a size distribution is added, particularly if the particle is anisotropically shaped and polydispersity of multiple dimensions (e.g. radius and length) is required.

The resolution function of the instrument, which depends on geometry and wavelength distribution for a pinhole SANS instrument, has a similar effect on the scattering curve and thus correct account must be made for those smearing effects if one is to extract the size distribution from a fit.

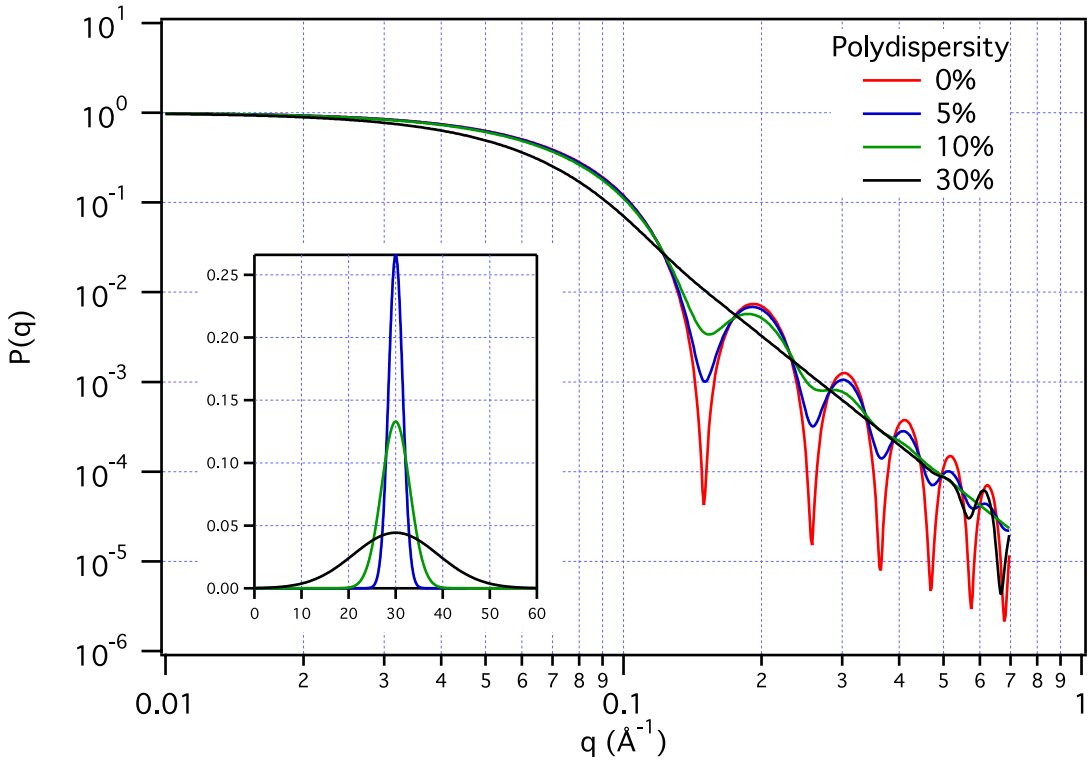

Figure 10: Form factor of spheres of radius 30Å with a distribution of radii. The polydispersities are $p = \sigma/R_{mean}$ quoted as a percentage. Size distributions for the non-zero polydispersites are inset.

5 Neutron Reflectometry

As mentioned in the introduction, neutrons obey the same laws as electromagnetic waves and as such display reflection and refraction on passing from one medium to another.

Whilst the reflection of neutrons as a phenomenon has been known since first reported by Fermi and co-workers in the late 1940's it is only relatively recently (1980's) that application of the technique as a structural probe was seriously considered. As we shall see, the reflection of neutrons is a powerful technique for the probing of surface structures and buried interfaces on the nanometer length scale.

The reflection of neutrons from surfaces is, however, very different from most neutron scattering. In the discussion of scattering theory and small angle scattering we assumed that we could calculate the scattering cross section by adding the scattering from each nucleus in the sample. This involved the assumption that a neutron is only scattered once on passing through the sample and is called the Born approximation.

We ignored multiple scattering because these effects are usually very weak. However, in the case of reflection close to and below the critical angle (where neutrons are totally reflected from a smooth

surface) we are no longer considering weak scattering and the Born approximation no longer holds. Thankfully we can use the constructs of classical optics to discuss the behavior of neutrons under these circumstances.

5.1 Specular Reflection

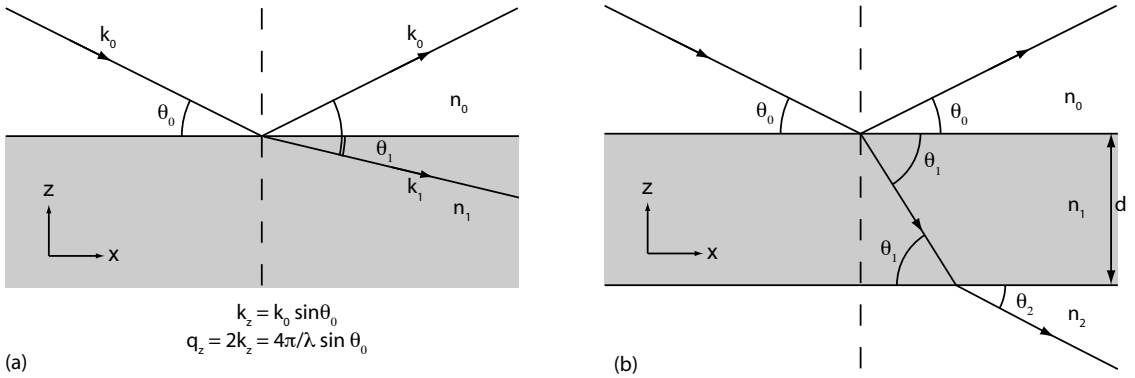

Figure 11: (a) The interface between two bulk media of refractive indices n_0 and n_1 showing incident and reflected waves at angle θ_0 and the transmitted wave at angle θ_1. (b) A thin film of thickness d and refractive index n_1 between two bulk media of refractive indices n_0, n_2.

Specular reflection is defined as reflection in which the angle of reflection equals the angle of incidence. Consider the neutron beam with wavevector k_0 in figure 11(a) incident on a planar boundary between media 1 and 2. The refractive index at the boundary between two media is defined as usual

$$n = \frac{k_1}{k_0} \tag{43}$$

where k_1, k_0 are the neutron wavevectors inside and outside the medium. The refractive index of a material against vacuum is commonly written as

$$n_i = 1 - \frac{\lambda^2 \rho_i}{2\pi} \tag{44}$$

where ρ_i is the scattering length density of medium i (as previously defined for SANS) and absorption has been ignored. Since usually $n < 1$, neutrons are externally reflected from most materials with Snell's law giving the *critical angle* below which total reflection occurs

$$\cos\theta_c = \frac{n_2}{n_1} \tag{45}$$

For neutrons incident on the surface of a material (e.g. water or silicon) from air (which has a refractive index very close to 1) we can obtain a simple relationship between the critical angle, neutron wavelength and scattering length density of the material

$$\theta_c = \lambda\sqrt{\frac{\rho}{\pi}} \tag{46}$$

It is important to note that the only change in wavevector is in the z direction (perpendicular to the interface) and hence a specular reflectivity experiment measures the scattered intensity as a function of $q_z = 2k_z$. As such, the reflectometry experiment provides information about structure perpendicular to the interface. It is possible to measure the reflection at non-specular angles to extract information about the in-plane structure of the sample. Such *off-specular* reflection is beyond the scope of this introduction so the reader is encouraged to consult the literature for more information.

5.1.1 Classical Optics

It has been shown that the same laws apply for the reflection and refraction of neutrons as for an electromagnetic wave with its electric vector perpendicular to the plane of incidence (s-wave). Thus the reflectivity is given by Fresnel's law where for $\theta \leq \theta_c$ the reflectivity $R = 1$ and for $\theta \geq \theta_c$

$$R = |r|^2 = \left| \frac{n_0 \sin\theta_0 - n_1 \sin\theta_1}{n_0 \sin\theta_0 + n_1 \sin\theta_1} \right| \tag{47}$$

The Fresnel calculation can be extended to the case of a thin film at the interface figure 11(b). A beam incident on such a system will be multiply reflected and refracted at the interfaces between the layers. Taking into account the phase changes that occur, the reflection and refraction coefficients for each pair of adjoining media may be calculated by an infinite sum of amplitudes of the reflected and refracted rays. For a single thin film of thickness d this leads to an exact equation for the interference from the film

$$R = |r|^2 = \left| \frac{r_{01} + r_{12} e^{2i\beta_1}}{1 + r_{01} r_{12} e^{2i\beta_1}} \right|^2 \tag{48}$$

where r_{ij} is the Fresnel reflection coefficient at interface ij given by

$$r_{ij} = \frac{p_i - p_j}{p_i + p_j} \tag{49}$$

with $p_j = n_j \sin\theta_j$ and $\beta_j = (2\pi/\lambda) n_j d \sin\theta_j$ (the optical path length in the film).

This approach can be extended easily to three or four discrete layers, but beyond that level of complexity a more general solution is required. One such standard method is that described by Born and Wolf where, on applying the condition that the wave functions and their gradients be continuous at each boundary, a characteristic matrix for each layer can be derived such that for the jth layer

$$\mathbf{M}_j = \begin{bmatrix} \cos\beta_j & -(1/p_j)\sin\beta_j \\ -p_j \sin\beta_j & \cos\beta_j \end{bmatrix} \tag{50}$$

The resulting reflectivity is then obtained from the product of the characteristic matrices $\mathbf{M}_R = [\mathbf{M}_1][\mathbf{M}_2] \ldots [\mathbf{M}_n]$ by

$$R = \left| \frac{(M_{11} + M_{12} p_s) p_a - (M_{21} + M_{22}) p_s}{(M_{11} + M_{12} p_s) p_a + (M_{21} + M_{22}) p_s} \right| \tag{51}$$

where M_{ij} are the components of the 2×2 matrix M_R.

Whilst the above calculations are only strictly valid for smooth interfaces between actual physical layers of material, one can imagine describing a layer of varying scattering length density as a series of layers of various scattering length densities. In the limit of infinite layers this would converge to an exact description of the scattering length density profile normal to the interface and thus correctly determine the reflectivity. This is, in fact, the way that the matrix formalism is mostly used (though with a lot less than infinite layers!). The question of smoothness needs to be addressed, however, and that is the subject of the next section.

5.1.2 Interfacial Roughness

Long range undulations, which can be considered locally flat, do not affect the above calculations. Here we consider variations from a completely smooth interface that occur on length scales of the same order as the neutron wavelength. Such local roughness modifies the specular reflectivity in a manner similar to a diffuse (non-sharp) interface and in fact the two are indistinguishable in the specular reflectivity experiment.

It can be shown that the presence of local roughness will modify the reflected intensity by a Debye-Waller-like factor such that

$$I(q) = I_0(q)e^{-q_0 q_1 <\sigma>^2} \tag{52}$$

where $I(q)$ and $I_0(q)$ are the reflected intensity with and without surface roughness, $<\sigma>$ is the root mean square roughness and $q_i = 2k\sin\theta_i$.

The above result is only valid for bulk interfaces. However it can be extended to interfacial roughness and diffuse interfaces of thin films by applying a Gaussian roughness factor to the Fresnel coefficients of each interface such that

$$r_{ij} = \left(\frac{p_i - p_j}{p_i + p_j}\right) e^{-0.5(q_i q_j <\sigma>^2)} \tag{53}$$

In order to use this result an alternative formulation of the matrix method is required that includes the Fresnel coefficients. Such a method is that of Abeles which defines the characteristic matrix for each layer as

$$\mathbf{C}_M = \begin{bmatrix} e^{i\beta_{m-1}} & r_m e^{i\beta_{m-1}} \\ r_m e^{-i\beta_{m-1}} & e^{-i\beta_{m-1}} \end{bmatrix} \tag{54}$$

For N layers the matrix elements M_{11}, M_{21} of the resulting matrix

$$\mathbf{M}_N = \prod_1^N \mathbf{M}_i \tag{55}$$

give the reflectivity

$$R = \frac{M_{21}M_{21}^*}{M_{11}M_{11}^*} \tag{56}$$

The roughness or diffuseness of the interfaces can now be introduced as above through the Fresnel coefficients.

It should be noted that it is not clear how the above roughness treatment - which applies a Gaussian factor to the reflectance - translates into roughness in the scattering length density profile. The

alternative is to describe the roughness or diffuseness of an interface by using a large number of very thin layers with a Gaussian distribution of scattering length density in equations (50) and (51). The treatment in equation (53) was preferred as it was much less computationally intensive. However, given the increase in computing power in recent years, it is probably now preferred to use the "exact" solution.

5.1.3 Kinematic (Born) Approximation

It was stated in the introduction to this section that the Born approximation does not hold because we are not in a weak scattering regime when critical reflection is concerned. However, if we look at high enough values of $\mathbf{q}$, then the scattering is weak and the Born approximation holds.

As for small angle scattering, the differential cross section is given by the Fourier transform of the scattering length density distribution over the whole sample. Taking into account the specular geometry such that only $\mathbf{q_z}$ varies we can obtain an expression for the reflectivity

$$R(\mathbf{q_z}) = \frac{16\pi^2}{q_z^2}|\hat{\rho}(q_z)|^2 \tag{57}$$

where $\hat{\rho}(q_z)$ is the *one-dimensional* Fourier transform of the scattering length density profile normal to the interface. This can also be expressed in terms of the scattering length density *gradient* thus

$$R(\mathbf{q_z}) = \frac{16\pi^2}{q_z^4}|\hat{\rho}'(q_z)|^2 \tag{58}$$

The above expression can then be used to calculate the reflectivity easily from a given scattering length density profile. Whilst it is limited to the weak scattering regime, there are many systems where this is valid. In particular the adsorption of molecules (e.g. surfactants, polymers) at the air-water interface where the scattering length density of the water can be set to match that of air. The validity can be extended to non-zero bulk contrast systems using the Distorted Wave Born Approximation or similar techniques.

6 Analysis of Reflectometry Data

The analysis of reflectometry data consists of generating a scattering length density profile, calculating the reflectivity using one of the methods described previously and comparing the result to the reflectivity profile obtained from experiment. An example of calculated reflectivity profiles is shown in figure 12

As a result of the loss of phase information on taking the magnitude of the Fourier transform, a given reflectivity profile can not be uniquely described by a single scattering length density profile. However this deficiency can be overcome through the use of multiple contrasts. Indeed, if one can measure the same system whilst changing *only* the scattering length density of either bulk side of the interfacial then the phase information can be recovered and the data inverted to get the SLD profile. This can be achieved by changing the solvent (e.g. by exchanging H_2O for D_2O) as long as

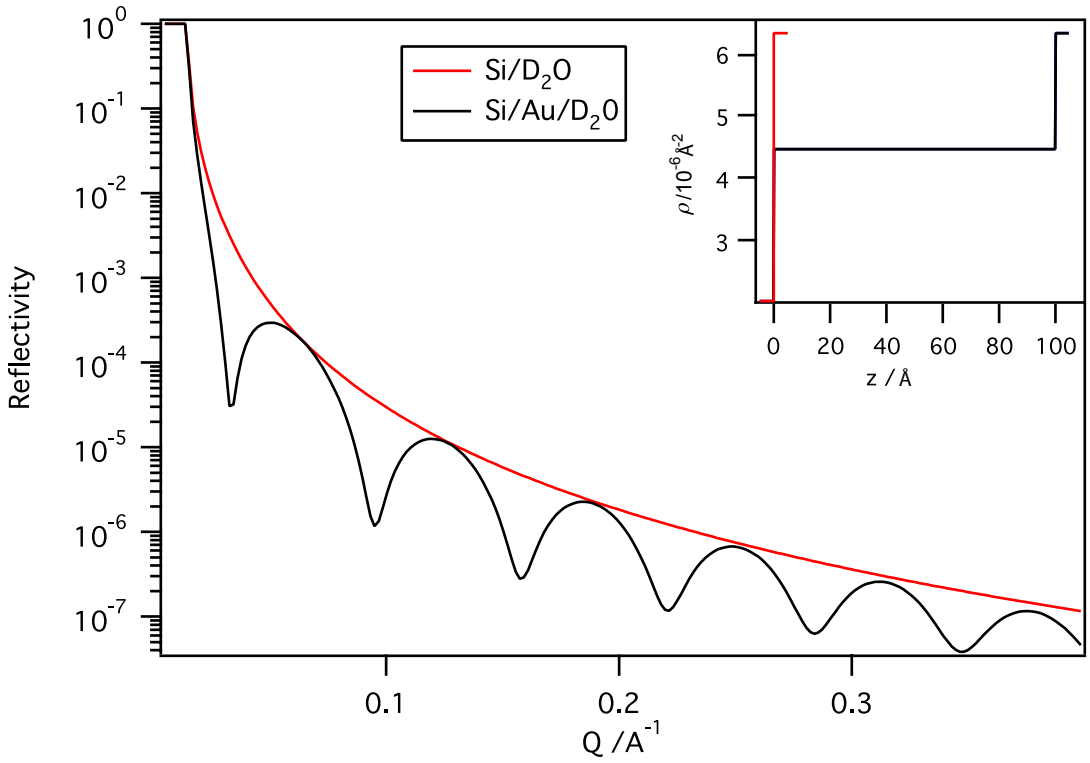

Figure 12: Calculated reflectivity profiles for a smooth D2O-Silicon interface (red curve) and a 100Å thick layer of gold on that surface. The Abeles method was used.

there is no solvent penetration into the interfacial layer or by using a magnetic reference layer and polarized neutrons to obtain two contrasts without changing the sample at all.

In practice this is often difficult and simultaneous fitting of multiple solvent contrast data is the only solution.

7 Recommended Reading

7.1 Neutron Scattering

"Neutron Scattering - A Primer" by Roger Pynn (LAUR-95-3840 Los Alamos Science, Vol. 19, 1990.)

`http://www.mrl.ucsb.edu/~pynn/primer.pdf`

"Introduction to Thermal Neutron Scattering" by G. L. Squires (Cambridge University Press, 1978) This is an excellent book if you want the nitty-gritty of scattering theory. It is now available from Dover Publications and at the time of writing is only $12 from Amazon.com

7.2 Small Angle Neutron Scattering

"The SANS Toolbox" by Boualem Hammouda - available as a PDF from the NCNR website.

`http://www.ncnr.nist.gov/staff/hammouda/the_SANS_toolbox.pdf`

The NCNR SANS website contains tutorials and tools relating to SANS as well as information about the NCNR SANS instruments.

`http://www.ncnr.nist.gov/programs/sans/`

7.3 Reflectometry

The NCNR Reflectometry website has tutorials and tools relating to reflectometry along with information about the NCNR reflectometry instruments.

`http://www.ncnr.nist.gov/programs/reflect/`

8 Acknowledgements

This introduction is an amalgam of material from a number of sources. The section on neutron scattering was based heavily on sections in Squires and Bacon and those two books (Squires in particular) will reward the dedicated reader. The section on small angle neutron scattering was based on a set of powerpoint slides presented by Steven Kline of the NIST Center for Neutron Research at previous summer schools. The section on neutron reflectometry was based on a 1990 review article by Bob Thomas of Oxford University and Jeff Penfold of the ISIS neutron facility.

9 References

These are various books and papers that relate to the material presented here and fall into the "extended reading" category. This is by no means an exhaustive list and the reader is encouraged

to explore the literature.

9.1 Scattering and Optics

G.E. Bacon *Neutron Diffraction*, Clarendon Press, 1955 (out of print)

M. Born and E. Wolf *Principles of Optics* 7th ed, Cambridge University Press, 1999

R.M. Moon, T. Riste, and W.C. Koehler. *Phys. Rev.*, 181(2):920, 1969.
Polarization analysis of thermal neutron scattering.

9.2 Reflectometry

J. Penfold and R. K. Thomas *J. Phys - Condensed Matter*, 2:1369, 1990.
A review of reflectometry.

T. L. Crowley *Physica A*, 195:354, 1993.
Use of the kinematic approximation for non-zero contrast systems.

L. Nevot and P. Crocé *Phys. Appl.* 15:761, 1980.
Interfacial roughness.

R. Cowley and T. Ryan *J. Phys. D: Appl. Phys.* 20:61, 1987.
Interfacial roughness.

C. F. Majkrzak and N. F. Berk, *Phys. Rev. B* 52, 10827 (1995).
Phase determination by use of a magnetic reference layer.

C.F. Majkrzak and N. F. Berk, *Phys. Rev. B.* 59:15416, 1998.
Phase determination by varying surrounding media.

A Radius of Gyration of Some Homogeneous Bodies

Sphere of Radius R

$$R_g^2 = \frac{3}{5}R^2$$

Spherical shell with radii $R_1 > R_2$

$$R_g^2 = \frac{3}{5}\frac{R_1^5 - R_2^5}{R_1^3 - R_2^3}$$

Ellipse with semiaxes a and b

$$R_g^2 = \frac{a^2 + b^2}{4}$$

Ellipsoid with semiaxes a, b, c

$$R_g^2 = \frac{a^2 + b^2 + c^2}{5}$$

Prism with edges A, B, C

$$R_g^2 = \frac{A^2 + B^2 + C^2}{12}$$

Cylinder with radius R and length l

$$R_g^2 = \frac{R^2}{2} + \frac{l^2}{12}$$

Elliptical cylinder with semiaxes a and b and height h

$$R_g^2 = \frac{a^2 + b^2}{4} + \frac{h^2}{12}$$

Hollow circular cylinder with radii $R_1 > R_2$ and height h

$$R_g^2 = \frac{R_1^2 + R_2^2}{2} + \frac{h^2}{12}$$